frontiers | Frontiers in Virology

BRIEF RESEARCH REPORT
published: 06 June 2022
doi: 10.3389/fviro.2022.908704

Mimiviruses Interfere With IκBα Degradation

*Juliana dos Santos Oliveira[1], Dahienne Ferreira Oliveira[2], Victor Alejandro Essus[1], Gabriel Henrique Pereira Nunes[1], Leandro Honorato[3], José Mauro Peralta[4], Leonardo Nimrichter[3], Allan Jefferson Guimarães[5], Debora Foguel[2], Alessandra Almeida Filardy[6] and Juliana R. Cortines[1]**

[1] Laboratório de Virologia e Espectrometria de Massas (LAVEM), Instituto de Microbiologia Paulo de Góes, Departamento de Virologia, Universidade Federal do Rio de Janeiro, Rio de Janeiro, Brazil, [2] Laboratório de Agregação de Proteínas e Amiloidoses (LAPA), Instituto de Química Biológica Leopoldo de Meis, Universidade Federal do Rio de Janeiro, Rio de Janeiro, Brazil, [3] Laboratório de Glicobiologia de Eucariotos, Institutode Microbiologia Paulo de Góes, Departamento de Microbiologia Geral, Universidade Federal do Rio de Janeiro, Rio de Janeiro, Brazil, [4] Laboratório de Diagnóstico Imunológico e Molecular de Doenças Infecciosas e Parasitárias (LaDIMDIP), Universidade Federal do Rio de Janeiro, Brazil Universidade Federal do Rio de Janeiro, Instituto de Microbiologia Paulo de Góes, Departamento de Imunologia, Rio de Janeiro, Brazil, [5] Departamento de Microbiologia e Parasitologia, Instituto Biomédico, Universidade Federal Fluminense, Niterói, Brazil, [6] Laboratório de Imunologia Celular, Departamento de Imunologia, Instituto de Microbiologia Paulo de Góes, Universidade Federal do Rio de Janeiro, Rio de Janeiro, Brazil

OPEN ACCESS

Edited by:
Sonia Zuñiga, Spanish National Research Council (CSIC), Spain

Reviewed by:
Philippe Colson, IHU Mediterranee Infection, France
Anthony Levasseur, Aix-Marseille Université, France

***Correspondence:**
Juliana R. Cortines
cortines@micro.ufrj.br

Specialty section:
This article was submitted to Fundamental Virology, a section of the journal Frontiers in Virology

Received: *30 March 2022*
Accepted: *16 May 2022*
Published: *06 June 2022*

Citation:
dos Santos Oliveira J, Oliveira DF, Essus VA, Nunes GHP, Honorato L, Peralta JM, Nimrichter L, Guimarães AJ, Foguel D, Filardy AA and Cortines JR (2022) Mimiviruses Interfere With IκBα Degradation. Front. Virol. 2:908704. doi: 10.3389/fviro.2022.908704

Many aspects of giant viruses biology still eludes scientists, with viruses such as Acanthamoeba polyphaga mimivirus (APMV) and Tupanvirus (TPV) possessing large virions covered by fibrils and are cultivated in laboratories using Acanthamoeba cells as hosts. However, little is known about the infectivity of these giant viruses in vertebrate cells. In the present study, we investigated the consequences of the incubation of APMV and Tupanvirus with mammalian cells. These cells express Toll-like receptors (TLR) that are capable of recognizing lipopolysaccharides, favoring the internalization of the antigen and activation of the inflammatory system. By using a lineage of human lung adenocarcinoma cells (A549), we found that APMV and TPV virus particles interact and are internalized by these cells. Furthermore, when treating cells with a fibriless variant of APMV, the M4 strain, there was no significant loss of cell viability, reinforcing the roles of fibrils in cell activation. In addition, we found an upregulation of TLR4 expression and an expected down regulation of IκBα in A549 APMV or TPV-infected cells compared to non-infected cells. Our results suggest that mimiviruses are able to interact with innate immune components such as TLR4, inducing their downstream signaling pathway, which ultimately active proinflammatory responses in lung cells.

Keywords: acanthamoeba polyphaga mimivirus, tupanvirus, fibrils, lipopolysaccharide, toll like receptors, IκβA

INTRODUCTION

The Acanthamoeba polyphaga mimivirus (APMV) was identified and classified as a new type of virus in 2003, with its discovery heralding a new era in virology. Among its many distinguishing features, the APMV possesses a pseudo-icosahedral capsid with a size nearing 500 nm in diameter. Its particle is almost entirely covered by fibrils (125 - 140 nm), save for the stargate, a feature that plays a role in

the liberation of the virion's internal contents, characterized by the presence of a star-shaped seal-like structure (1–7). Subsequent searchs led to the discovery of the Tupanviruses (TPV), which were isolated in 2018 in Brazil. Similar to APMV, they are members of the *Mimiviridae* family, with currently only two known strains: Tupanvirus-Soda Lake (TPV-SL) and Tupanvirus-Deep Ocean (TPV-DO), that compose the *tupanvirus* genus. Similar to the APMV, it possesses a capsid with pseudo-icosahedral geometry near 450 nm in diameter, almost totally covered in fibrils, and presents the stargate in one of its vertices (8). A unique aspect to TPV virion is the presence of a long cylindrical tail at the opposite side from the stargate vertex that portraits variable lengths and is also covered by fibrils (8).

Although their function is still unknown, it is believed that fibrils play an important role in GVs infection cycles. They are found in almost all the known GV families (3). Data obtained through atomic force microscopy shows that the APMV capsid surface is coated by a protein matrix with high levels of sugar. Peptidoglycan protrusions might act as anchoring points for the fibrils and in their protection (9, 10). Although the characterization of the fibril matrix has yet to be completed, the existence of peptidoglycans is sustained by the APMV susceptibility to Gram coloration, and due to the presence of the *L136* gene (11, 12). This gene encodes an enzyme that acts in the synthesis of viosamin, a monosaccharide found in the O-antigen subunit of the lipopolysaccharide (LPS) of many bacterial strains. It was also evidenced by the presence of rhamnose in the fibrils, another monosaccharide present in bacterial LPS (11, 13). The fibrils are disposed in a dense layer along most of the virion surface, in the case of the members of *Mimiviridae* family. It is worth mentioning that a fibreless mutant of APMV known as Mimivirus M4 was obtained through repeated culturing, with this variant presenting a drastic reduction to its genome size. Large genomic sections were deleted including genes associated with the expression of proteins involved with the biosynthesis of carbohydrates and structural proteins that form the fibrils (14, 15). Although lacking the fibrils, they are still capable of infecting cells and replicating, albeit at a slower pace (14, 16). This fact reinforces that the fibrils play an important role in the infection cycle. They seem to act in the virus-cell contact, which makes them more attractive for professional phagocytes, such as amoebas (16).

The large size of these viruses (> 500 nm) led to the theory that, in the vast majority, their replicative cycles were dependent on the virus-cell entry through phagocytosis (17). In fact, professional phagocytic cells such as certain amoebal trophozoites with intense phagocytic activity are the main GVs hosts used in laboratory (7, 18, 19). However, the intricacies of GV internalization by amoebas are still unknown. It's thought that certain portions of the capsid or fibrils of APMV or TPV can activate cellular receptors that trigger cytoskeleton changes, allowing for the phagocytosis of the virions (17, 20). In humans, the phagocytic process can be undertaken by professional (i.e., macrophage), non-professional (i.e., epithelial cells) and specialized (i.e., Sertoli testicle cells) phagocytic cells (21). The similar structural aspects between the fibrils and bacterial structures can be related to the host cellular response, since LPS, bacterial membrane structures and viral components can activate receptors from the Toll-like (TLRs) family (22).

The TLR family of receptors is responsible for the identification of pathogen-associated molecular patterns (PAMP), being present in the front line of the innate immune system response (22). Toll-Like Receptors 4 (TLR4) are proteins composed of intra- and extracellular domains located in the membrane of different types of cell, including the pulmonary alveolar epithelium (23). These are sensitive to the presence of LPS, and when activated can trigger two signaling pathways: one dependent on the primary response protein of the myeloid differentiation primary response 88 (MyD88) and the MyD88 independent pathway. In the first pathway, the IRAK4 kinase (interleukin-1 receptor-associated Kinase 4) suffers phosphorylation and activates IRAK1 (interleukin-1 receptor-associated kinase 1). The complex formed by MyD88 and the interleukin 1 and 4 recruit TRAF6 (TNF receptor-associated factor 6) so that the complex TAK1 (TGFβ activated kinase 1) and TAB2 and 3 (TAK1 binding protein) can activate the kinases IKKα, IKKβ and IKKγ. These three kinases promote the IκB phosphorylation and its degradation allows the translocation of the nuclear factor-κB (NF-κB) to the nucleus, and the production of inflammatory cytokine. The MyD88 independent pathway needs adaptor molecules TRIF (TIR domain containing adapter protein inducing interferon IFN-β) and TRAM (TRIF-related adaptor molecule) to activate a distinct set of transcription factors (23, 24). Based on the role these types of receptors have in the cellular immune response and the identification of antigens such as LPS, it is possible that it is involved in the cellular response to GVs.

Further highlighting the possible immunogenicity of GVs are previous serological tests and western blot assays in samples from pneumonia patients and infection tests with mice. They showed the presence of specific antibodies and viral proteins for APMV and other members of the *Mimiviridae* family (25–27). As such, it is paramount that the possible impacts these viruses can have in humans be extensively explored. In this context, the present work evaluates the propensity of the APMV and TPV-SL internalization by adenocarcinomic human alveolar basal epithelial cells (A549). This cell line was chosen due to serving as an excellent model of alveolar epithelium type II. We also evaluated changes in TLR4 expression and IκBα degradation in cells kept in the presence and/or absence of different multiplicity of infection of APMV and TPV. Since APMV and TPV fibrils can be composed of protein content similar to LPS, it is suggested that short incubation periods can be enough to cause a response from both of these indicators, resulting in an important inflammatory process.

MATERIALS AND METHODS

Viral Particles' Purification

Three million *Acanthamoeba castellanii* cells (strain 30011) were grown in 75 cm^2 cell-culture flasks and maintained in Peptone,

Yeast Extract and Glucose medium (PYG, ATCC Medium 712) containing 1 mg/ml penicillin/streptomycin (Sigma-Aldrich, USA) and 15 μg/ml gentamicin (Thermo Fisher Scientific, USA) for one hour. After complete adherence, the amoebas were infected with APMV, Mimivirus M4 or TPV- soda lake (TPV-SL was used for all experiments in the present work) at a multiplicity of infection (MOI) of 0.5 and stored in an oven at 28 °C. After 96 hours of infection, the collected cell lysate was carefully placed in 22% sucrose cushion, and centrifuged at 36,000 ×g for 30 min. The resulting viral pellets were resuspended in 500 μL of sterile PBS. Virus titers were determined using the method of Reed and Muench (28). On average, purification of APMV yielded titers of 10^8 TCID50/ml, Mimivirus M4 of 10^7 TCID50/ml and TPV of 10^7 TCID50/ml. The APMV and M4 samples were a kind gift from Bernard La Scola, while the TPV -SL were generosly donated by Jonatas Santos Abrahão.

Labeling of Viral Particles

APMV and TPV-SL stocks at the desired MOI were centrifuged (25,000 xg, 10 min, 4°C) and the viral pellet was separated. Rhodamine-phalloidin (25 μg/ml) diluted in 1 ml of sterile PBS was filtered in a 0.22 μm filter and added to the desired virus pellet. The pellet was then resuspended in this marking solution and submitted to orbital shaking (Phoenix Technologies) for 1 h at room temperature. Unbound rhodamine was removed by 5 washes with 1 ml of sterile PBS, after centrifugation under the conditions cited above. The resulting pellet was resuspended in PBS in the original stock volume.

Cell Culture

The A549 cell line (ATCC CCL-185) derived from human lung adenocarcinoma cells was chosen to carry out this work. Cells were grown in 75 cm^2 cell culture flasks, maintained in Dulbecco's Modified Eagle's Medium (DMEM - Sigma Aldrich), supplemented with 10% fetal bovine serum plus 1% gentamicin and stored in an incubator containing 5% CO2 at 37°C. Culture medium exchange was performed 2-3 times per week. In experiments in-volving polymyxin B (Sigma Aldrich, USA), cell cultures were previously treated with 50 μg/ml of this compound for one hour. Soon after this incubation, A549 cells were immediately exposed to DMEM, LPS (100 ng/ml), APMV (MOI 50) or TPV (MOI of 10 or 50).

Confocal Fluorescence Microscopy

Ten thousand A549 cells were plated in 24-well plates. After 24 hours, the cells were incubated with TPV (MOI of 10 or 50) and APMV (MOI of 50) for 6 hours and kept in DMEM for another 36 hours. Then, the cells were fixed on coverslips present in 24-well plates, with 4% paraformaldehyde for 15 minutes at room temperature. Cells were blocked with 5% BSA, in PBS pH 7.4 for 1 hour, followed by the incubation with fluorescein isothiocyanate (FITC)-cholera toxin B subunit (CTB; Sigma, USA, 1: 1000 diluted in sterile PBS) for 1 hour at 4°C, washed 3x with PBS and then incubated with DAPI (1:5000) for 15 minutes, washed again 3x with PBS and mounted with Prolong® on slides for microscopy analyses. Images were acquired with a Leica TCS-SPE confocal microscope equipped with an oil immersion objective 63× and a Nikon DS-fi2 camera operated with standard QC capture software (Leica, USA). Image analysis was done using the ImageJ program.

Scanning Electron Microscopy (SEM)

For scanning electron microscopy analysis $5x10^4$ A549 cells were cultured in round glass coverslips treated with laminine (1h) and previously placed inside the 24 wells culture plate. After 24 hours, cells were exposed to APMV, Mimivirus M4 and TPV at MOI 50 and incubated for 5 hours. Subsequently, samples were fixed using glutaraldehyde 2,5% in cacodylate buffer 0.1 M for 1h in room temperature. The samples were washed with a cacodylate buffer (0.1 M) three times and incubated with 1% osmium tetroxide for 1 h at room temperature. Later, cells were again washed three times with cacodylate buffer (0.1 M) and then dehydrated using ethanol solutions (35, 50, 70, 85, 95, and 100%) in 10 minutes treatments each. Samples were then led to the chemical critical point and metalized with a 5 nm gold coating. For sample visualization Scanning/Scanning-Transmission Electron Microscopy - Tescan VEGA 3 LMU, at the Núcleo Multidisciplinar de Pesquisa em Biologia (NUMPEX-BIO UFRJ) and Zeiss EVO 10 at the Unidade de Microscopia Avançada do Centro Nacional de Biologia Estrutural e Bioimagem (UMA-CENABIO).

Protein Expression Analysis by Western Blotting

The expression of TLR4 and IκBα proteins were analyzed using Western blotting assays. Cultures of A549 cells, containing 10^6 cells/well in six-well plates, were incubated with APMV (MOI 50) or TPV (MOI 10 or 50) and LPS (100 ng/ml) for 30 minutes. The proteins were separated by Sodium dodecyl sulfate Polyacrylamide gel electrophoresis (SDS-PAGE) and transferred to polyvinylidene fluoride membranes (Millipore). The membranes were incubated with mouse antibodies directed against TLR4 (ab22048, 1:1000 diluted in Odyssey buffer, abcam) and IκBα (Cat #: 9247, 1:1000 diluted in Odyssey buffer, Cell Signaling Technology). After incubation with the respective secondary mouse antibodies (IRDye,680 Licor, USA) immunoreactive signals were detected by Fluorescence. Fluorescence was measured with Odyssey FC Imaging System (Licor). Bands densitometry were normalized using GAPDH as a loading control. Statistical analysis was done using the Student T test. The data was evaluated as a ratio of the target proteins and the relative expression of the control protein. Statistical significance was confirmed when $p \leq 0,05$.

RESULTS

A549 Cells Interact and Internalize APMV and TPV Virus Particles

A549 cells are an excellent model to study respiratory infections, since they can work as replication platforms for viral pathogens that cause these infections. In this scenario, we inferred whether these cells could interact with and support GV replication.

Through SEM or fluorescence microscopy, we analyzed the ability of A549 cells to interact with APMV, Mimivirus M4, and TPV-SL. Through the images obtained by SEM, it was possible to observe that all viruses adhered to the cell surface (**Figure 1**). For fluorescence microscopy, we kept the cell cultures in contact with rhodamine labeled APMV (MOI 50) or TPV (MOI 10 or 50) for six hours, then replaced by DMEM supplemented with calf serum and antibiotics, for 36 hours more. Confocal microscopy images (**Figure 2** and in **Supplementary Figures 1–4**) show that the particles of APMV and TPV-SL are internalized by this cell line. We observed that, upon exposition of cells to APMV at an MOI of 50, a great quantity of viral particles appear to be co-localized with the cell membrane (**Figures 2A, B**). The same was observed when cells exposed to TPV in MOI of 10 and 50, respectively (**Figures 2C, D**). The number of viral particles along the cells increased proportionally to the increase in MOI used, as can be seen by the increasing number of red dots in the microscopies. For simplicity, we considered each dot to be a single particle. When counted, there were a total of 352 dots in the samples exposed to APMV at MOI of 50 (**Figure 2B**), 34 and 447 dots in samples exposed to TPV at MOI 10 (**Figure 2C**) and 50 (**Figures 2D, E**). The increase of over 10x in the numbers of dots between the MOIs used in the TPV sustains the observation of the proportional increase between MOI and virus entry. We also observed overlapping points of viruses with the nucleus, but it cannot be confirmed whether there was an invasion of such organelle. To date, there is no data that would support such observation. The co-localization of both viruses on the cell membrane is strong evidence that the cell-virus contact occurred. Also suggests that the fibrils are recognized by cell receptors, since interaction with them would enable adhesion and internalization and the fibrils are the outermost structure of the virion making it the most likely to engage in such activity. These observations suggests that A549 cell lines are susceptible to GVs.

A549 Cells Are Responsive to APMV and TPV Fibrils

In order to better understand the cells response after exposure to GVs, we sought to assess whether the presence of APMV or TPV would activate TLR4 receptors on A549 cells. Due to the similarities between fibril and LPS composition, we theorized that giant virus-A459 interaction could trigger TLR4 activation. First, we evaluated TLR4 expression in A549 cells exposed to APMV (MOI 50) or TPV (MOI 10 or 50) through immunoblotting assays (**Figures 3A, B**). TLR4 protein expression was detected in A549 stimulated with LPS, TPV or APMV viruses (**Figures 3A, B**). In this experiment, we also used polymyxin B (Poli-B), a cationic antimicrobial polypeptide that inactivates LPS by binding to the lipid A portion of the antigen, inhibiting its activity. The cultures were treated for one hour with 50 μg of polymyxin B and then TPV (MOI 10 or 50), APMV (MOI 50) or LPS (100 ng/ml) were added for 30 minutes. We found an increased TLR4 protein expression in the cell samples incubated with both viruses TPV and APMV as well as with LPS, compared to the unstimulated control cells. In samples exposed to APMV and TPV-SL, the TLR4 band intensity increased ~2.2x for APMV, and ~2.3x or ~3.8x for TPV at MOI 10 or 50, respectively. The cell samples exposed to LPS alone showed a

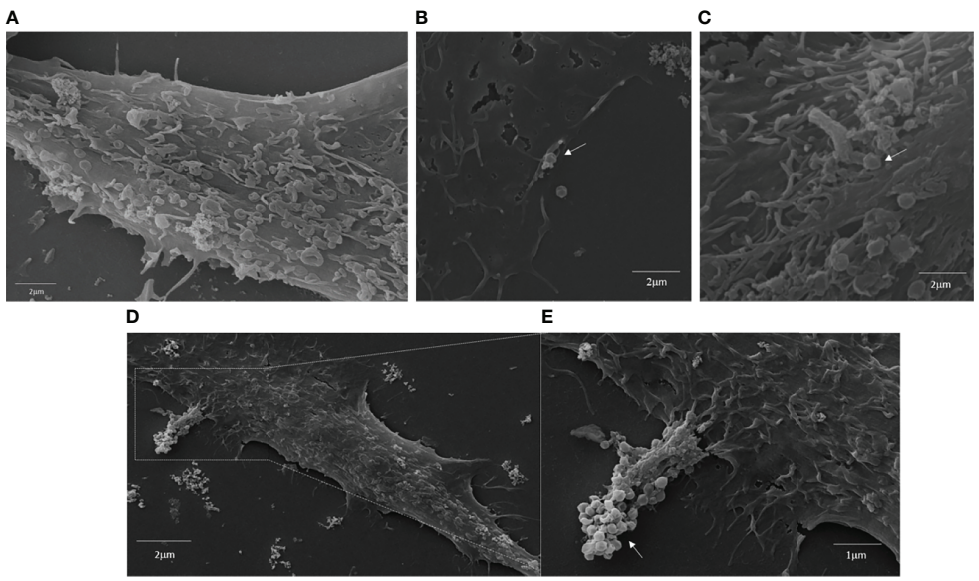

FIGURE 1 | Interaction of APMV, TPV and Mimivirus M4 with A549 cells membranes. A549 cells were incubated with APMV (MOI of 50) TPV (MOI of 50) and Mimivirus M4 for 6 hours at 370C. The samples were then prepared for Scanning Microscopy (see Scanning electron microscopy (SEM) section of materials and methods). **(A)** Cell in DMEM, Scale bar: 2 μm, **(B)** Cells incubated with APMV (MOI 50), Scale bar: 2 μm, **(C)** Cells incubated with TPV (MOI 50), Scale bar: 2 μm and **(D, E)**, Cells incubated with Mimivirus M4 (MOI 50), Scale bar: 2 μm and 1μm. White arrows signal the presence of GVs.

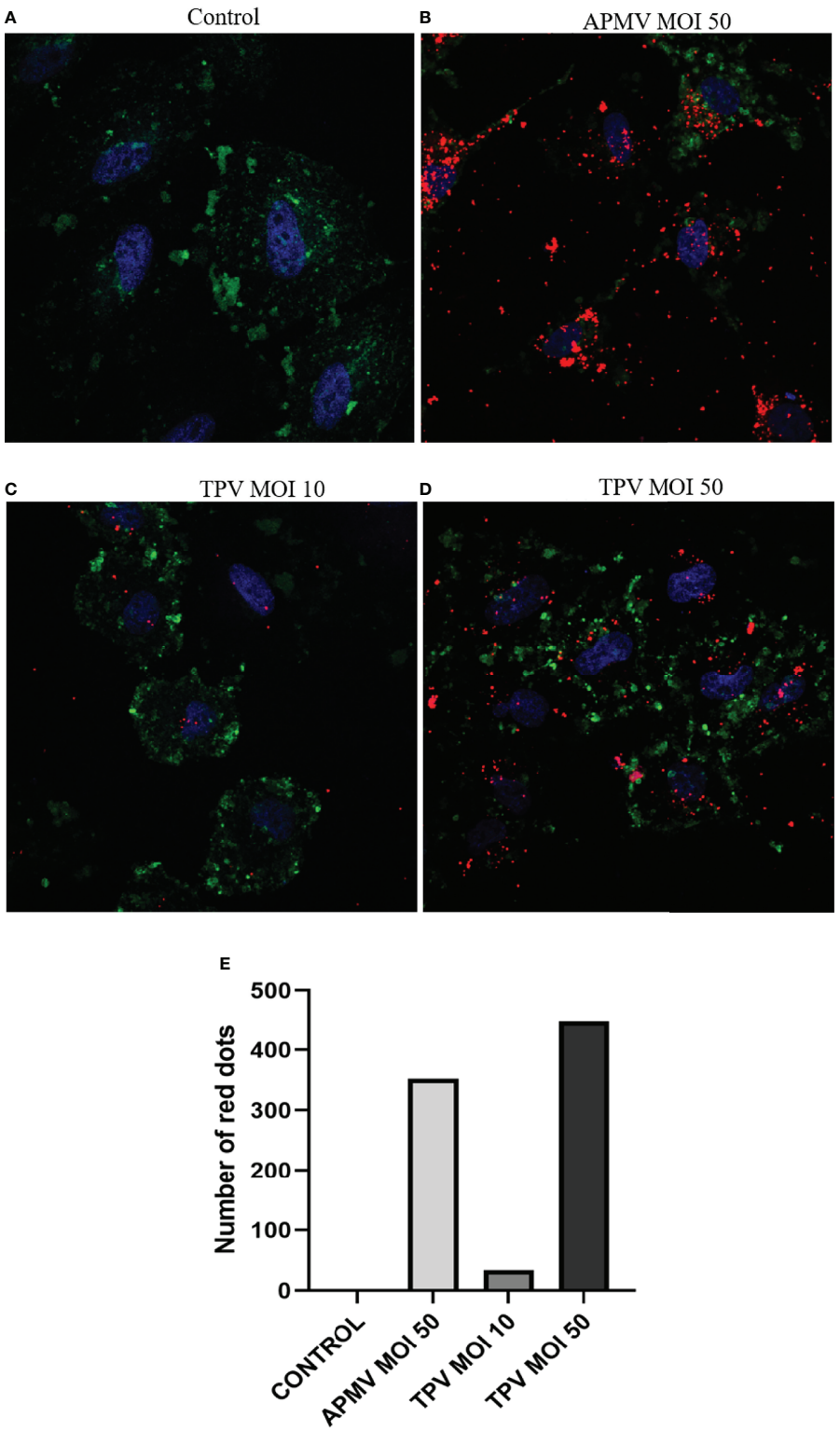

FIGURE 2 | Interaction of APMV and TPV with A549 cells after 36 hours. Fluorescent microscopies showing the A549 cells invasion by rhodamine-phalloidin-labeled APMV and TPV (red). A549 cells were incubated with APMV (MOI of 50) and TPV (MOI 10 or 50) for 6 hours, and labeled with FITC-CTB (green cell membrane) and DAPI (blue-core). **(A)** Cell in DMEM, **(B)** Cells incubated with APMV (MOI 50), **(C)** Cells incubated with TPV (MOI 10) and **(D)** Cells incubated with TPV (MOI 50). Scale bar: 10 µm. **(E)** Graph representing the number of APMV and TPV particles (red dots) internalized by cells.

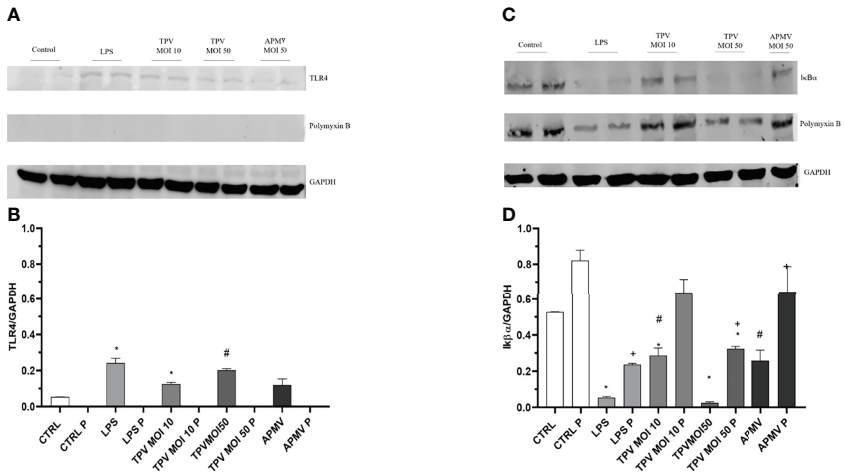

FIGURE 3 | Pulmonary epithelial cells TLR4 are weakly recruited and the degradation of IκBα was favored by the presence of APMV and TPV, regardless of the MOI used. Polymixin B completely blocks the activation of TLR4 and decreases the degradation of IκBα. **(A)** Representative immunoblot membrane that shows the weak TLR4 protein expression in A549 cells exposed for 30 minutes to DMEN, APMV (MOI 50), TPV (MOI 10 or 50), LPS (100 ng/ml), pretreated or not with polymyxin B (50 μg/m) for 1 hour. To confirm a similar gel load, the membranes were subjected to an anti-GAPDH antibody for two hours. **(B)** Graphic created using the ImageJ processing software the quantification levels of protein expression were made. The data was evaluated as a ratio of the target proteins and the relative expression of the control protein. **(C)** Representative immunoblot membrane demonstrating the absence of IκBα protein expression in A549 cells exposed for 30 minutes to DMEN, APMV (MOI 50), TPV (MOI 10 or 50), LPS (100 ng/ml), pretreated or not with polymyxin B (50 μg/m) for 1 hour. To confirm a similar gel load, the membranes were subjected to an anti-GAPDH antibody for two hours. **(D)** Graphic created using the ImageJ processing software the quantification levels of protein expression made. Student T test was used to determine the statistical significance comparing it with the control: p ≤0,05 *, p ≤0,05 #, p ≤0,05 *, p ≤0,05 #, p ≤0,05 +.

TLR4 expression increase of ~4.5x. In addition, we observed that TLR4 protein expression increased proportionally with MOI, where TPV at MOI 50 had similar detection as pure LPS (3.8 vs 4.5, respectively) (**Figure 3B**). On the other hand, polymyxin B pretreatment inhibited TLR4 expression in A549 cells treated with LPS, APMV or TPV (**Figures 3A, B**). These results so far suggest that surface structures of these viruses, that are rich in saccharides, i.e., the fibrils, have molecular similarity among the viruses as well as with bacterial LPS; and play an important role regulating TLR4 protein expression in eukaryotic cells.

TLR4 activation triggers a signaling cascade that culminates in IκBα phosphorylation and degradation (29). To investigate whether APMV and TPV activate TLR4 signaling pathway in A549 cells, we evaluated IκBα protein degradation by immunoblotting (**Figures 3C, D**). We found a decreased expression of IκBα in A549 cells stimulated with LPS and TPV at the MOI 50 compared to the unstimulated cells or in cells stimulated with TPV at the MOI 10 or APMV at the MOI 50, suggesting greater activation of the TLR4 pathway. The pretreatment with polymyxin B induced an inhibition in IκBα degradation in cells stimulated with different viruses as well as with LPS (**Figure 3C**). For samples stimulated with the viruses or LPS, the decrease in IκBα expression was ~0.42x and ~0.94x for TPV (MOI 10 and 50 respectively), ~0.49x for APMV (MOI 50), and ~0.89x for LPS. For the samples pretreated with polymyxin B, we found a decrease of 0.17x and 0.2x for TPV (MOI 10 and 50 respectively), 0.17x for APMV (MOI 50), and 0.32x for LPS, in IκBα expression (**Figure 3D**). Together, these results suggest that TPV and APMV virus structures bind to TLR4, activating the MyD88 pathway that ultimately, culminates in IκBα phosphorylation and degradation.

DISCUSSION

In this study, we demonstrate for the first time that human type II pneumocytes (A549) can establish adsorptive interactions with members of two genera of GVs, generating an immunological response. It is important to highlight that epithelial cells act strongly in the maintenance of systemic homeostasis, whether by phagocytizing dead cells or pathogens (30). As such, they are important agents in the innate immune response with the mechanics by which they capture the pathogen being an important factor of their efficacy (21). In this context, Chang and collaborators (2020) performed comparative assays of internalization of the bacterium *Klebsiella pneumoniae* (Kp) between macrophages (RAW 264.7) and A549 cells. Their data makes it clear that although epithelial cells can internalize Kp, the process is slow and continuous and therefore dependent only on the time of contact with the pathogen. Macrophages, on the other hand, internalized Kp in less time but in a limited way, that is, although bacteria were added to the medium, the internalization rate underwent little change (31). This difference can be explained by the absence of specific receptors aimed at phagocytosis in non-professional phagocytic cells, the process being entirely dependent on the pathogen's virulence factors (21, 30, 31). These aspects of phagocytosis in non-professional phagocytic cells are reflected in our results. Here,

we observe the adhesion (**Figure 1**) and internalization (**Figures 2B–D**) of the APMV, Mimivirus M4, and TPV viruses by A549 cells, and we suggest that this internalization may have occurred by phagocytosis, based on information available in the literature (21, 32). We suggest that this internalization may have occurred by phagocytosis, based on information available in the literature, where A549 cells were observed being capable of internalizing apoptotic cells and bacterial cells through phagocytosis (21, 31, 32), and this process being believed to be the main entrance route for GVs due to its size (17).

In our experiments, we allowed the virus to be in contact with the cells for six hours, and we observed a low uptake in samples that received TPV with MOI 10 (**Figure 2C**) when compared to cells incubated with APMV or TPV with MOI 50 (**Figures 2B, D**). As the process of internalization of pathogens by epithelial cells is slow and continuous (31), a greater number of particles can be internalized with a longer incubation time, even using viruses with a lower MOI. Another interesting observation is the fact that as the MOI increased, so did the number of internalized particles, evidenced by the increase of labeled virus signal in confocal microscopy images (**Figures 2B, D**). This might support the thesis of internalization mediated by phagocytosis due to the high number of particles in these titers not saturating viral entry, which is in accordance with the A549 cells internalization behavior previously described. This indicates that it is likely not one specialized receptor behind the capture, but that different non-specific receptors are acting in the process. Previous work has shown the importance of fibrils in APMV cell adhesion, through recognition of viral carbohydrates by amoeba cellular receptors (16). The study tested infection in mediums saturated with different kinds of sugar and observed that virus internalization rates were lower than in non-saturated mediums, especially in the presence of mannose. These data indicate that the sugar present in the medium competes with viruses for the cell receptor associated with viral adhesion (16), thus it's quite likely that non-specific receptors are associated with viral entry. However, it is necessary to perform further investigation to more consistently support such hypothesis.

Importantly, although internalization occurred, no sign of viral replication was observed. The lack of occurrence of cytopathic effect or formation of viral factories, normally associated with GVs infection in amoebas (2, 3, 7, 8, 18) suggests that no replication is occurring. Furthermore, the inability to purify virus particles from the infected pneumocytes strongly corroborates this observation. When put together, this information supports the failure to obtain viral particles in A549 cells incubated with APMV or TPV. It is also possible that, if any replication occurs in the interior of A459 cells, the dynamics of infection may be different, as we were not able to detect the viral factory in the images acquired. Interestingly, although it cannot be attested the occurrence of viral replication, loss of cell death was observed (**Supplementary Material**) although the causes are still unknown. To understand these cytotoxic effects, we evaluated the cell viability after the interaction of A549 cells with GVs using unlabeled TPV, APMV or Mimivirus M4 at MOIs of 0.1, 1, 10 and 50. All treatments resulted in cell death, with an increase in cell loss being proportional to the increasing number of GVs particles used (**Supplementary Figures 5, 6**). However, loss of viability varied in intensity between the viruses with TPV being the most toxic, as cultures exposed to an TPV MOI of 10 lost ~30% of viability, increasing to 40%-50% in MOI of 50 (**Supplementary Figure 5E**). When incubated with APMV at MOI of 10 it was observed a 27% loss of cell viability that increased to 33% in MOI of 50 (**Supplementary Figure 6A**). On the other hand, Mimivirus M4 showed the lowest toxicity of around 8% for MOI of 10 and 10% at MOI of 50 (**Supplementary Figure 6B**). Although some cell death was observed for Mimivirus M4, it was significantly reduced when compared with APMV. This difference most likely is due to the absence of fibrils on Mimivirus M4 particles, which reduces its phagocytosis by the cell. The proportional increase in cell death to the MOI utilized supports the hypothesis that the virus particle has a toxic effect over the cells.

Strong inflammatory response mediated by TLR4 is associated with cellular toxicity (33), which might be related with the observed cellular death as our results indicate that GVs can trigger this pathway (33–35). The literature has shown that A549 cells have both TLR4 and MD-2 mRNA expression. Generally speaking, the lipopolysaccharide binding protein (LBP) binds and transfers LPS to CD14. The CD14 protein has the function of transferring LPS to the MD-2 protein (a glycoprotein that is associated with TLR4). The MD-2/LPS interaction causes a structural change in the TLR4/MD-2 complex, which allows the release of NF-kB *via* the MyD88-dependent pathway (36, 37). We know that APMV fibrils have carbohydrates in their composition and some of these are also found in bacterial surface structures, such as LPS. Examples of such shared carbohydrates include rhamnosamine and viosamine (11, 13). Similar to APMV, TPV also has fibrils on its surfaces that in turn also have polysaccharides in their composition, although, different from APMV, their composition has yet to be determined. Therefore, our hypothesis is that these surface structures of APMV and TPV present structural similarities that are capable of triggering TLR4 activation, most likely by mechanisms similar to those of bacteria. This hypothesis is corroborated by the observation that both the addition of bacterial LPS and the maintenance of the virus in culture for 30 minutes initiate the increase in TLR4 expression (**Figures 3A, B**). These results support not only the hypothesis that they activate the TLR4 signaling pathway, but also further poses the notion that both viruses' fibrils possibly share some structural similarity to bacterial LPS. The small increase in TLR4 expression in the presence of LPS or viruses may be related to the low availability of CD14 in this cell line. Previous studies reported that A549 cells, unlike macrophages, have little expression of membrane CD14, requiring the addition of this protein to the culture through the supplementation of fetal bovine serum (38). On the other hand, cells treated with the LPS inhibitor (Polymyxin B) were protected from the action of LPS and viruses, since, in this case, there was no increase in TLR4

protein expression (**Figures 3A, B**). The results obtained for the IκBα protein points in the same direction as the previous experiment. The IκBα degradation pathway, activated by the interaction of LPS with TLR4, also seems to be stimulated by TPV (MOI 50) and, to a lesser extent, from exposure to TPV (MOI 10) and APMV (MOI 50) (**Figures 3C, D**). Another important study evaluating innate immune response to mimiviruses (39, 40) offered an in depth look into interferon production triggered in peripheral blood mononuclear cells (PBMCs) by GVs exposure. They observed the presence of type I IFN (IFN-α2 and IFN-β) mRNAs in PBMCs after 18 hours of infection implying that APMV infection does not interfere in the INF production pathways. However, the INF response route was compromised due to the absence of ISGs, even though the phosphorylation of STAT1/STAT2 was not affected. Therefore, their results indicate that APMV is capable of evading the cell's immune response by blocking the INF response in a yet unknown mechanism. Our findings complement this elegant study as we explore the APMV and TPV interaction with TLR4, also associated with the LPS detection, indicating a probable signaling pathway triggered by the GVs. Under these circumstances the interferon is a product of the translocation of NF-κB to the nucleus *via* IκBα degradation. As such, we believe that our data indicates that APMV and TPV fibril composition could be detected by TRL4 similarly to LPS.

In conclusion, this work reinforces the peculiarity of the interaction between GVs and human cells, as summarized in the **Figure 4**, as well as of these viruses' structures. We showed that upon interaction with mimiviruses, mammalian cells recognize viral structures, mostly *via* fibrils, triggering a TLR mediated MyD88 signaling cascade. This pathway leads to the IκBα degradation (**Figures 3C, D**) and release of NF-κB to the nucleus, resulting in the expression of proinflammatory cytokines. Previous genomic and proteomic studies based on data obtained from genome sequencing show that mimiviruses possess genes related to organisms present in each of the three domains of life. This amazing aspect reinforces the possible evolutionary relationships of the GVs with bacterias, archeas, and eukaryotes. Such data can help enlighten the similarities observed in structural composition, and how these structures can be related with infection mechanisms or the activation of cytotoxic response in different cell types (4, 8, 41). The results shown here reinforce such correlation, as both APMV and TPV appear to trigger the TLR4 response similarly to the LPS, most likely due to structural similarities. Our results serve as a base to further explore this very complex relationship.

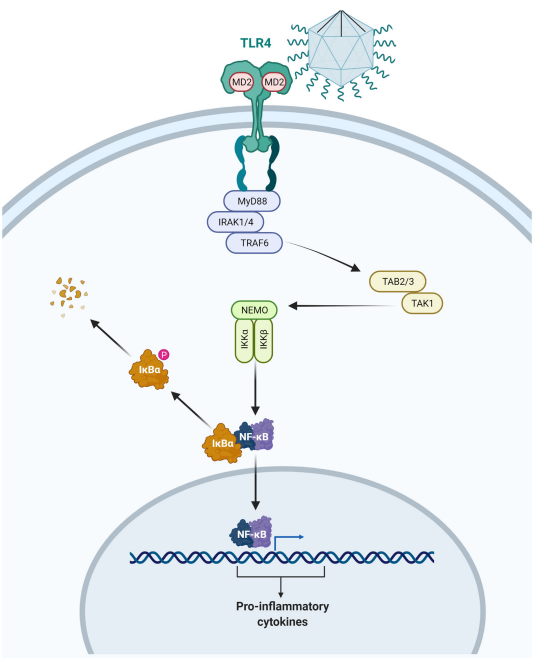

FIGURE 4 | Illustration representing the activation of the myeloid 88 dependent TLR4 pathway by contact with the APMV. Following the TLR4 activation, the IRAK4 kinase suffers phosphorylation and activates IRAK1 resulting in TRAF6 recruitment. This allows the TAK1 and TAB2/3 complex to activate the kinases IKKα, IKKβ, and IKKγ. These enzymes promote the IkB phosphorylation and its degradation allows the translocation of the nuclear factor-kB (NF-kB) to the nucleus, and the production of inflammatory cytokine. This representation is merely illustrative and is not up to scale. Drawing created with BioRender.com.

DATA AVAILABILITY STATEMENT

The datasets presented in this study can be found in online repositories. The names of the repository/repositories and accession number(s) can be found in the article.

AUTHOR CONTRIBUTIONS

JDSO performed experiments and wrote the manuscript. DFO performed experiments. VAMSAE helped in the discussion of the results, revised the manuscript and drew the illustration. GHPN, JRC, and AAF revised the manuscript. LH, LN, JMP, AJG, and DF helped in the development of the experiments. All authors contributed to the article and approved the submitted version.

FUNDING

JDSO, DFO and GHPN received a PhD fellowship provided by Conselho Nacional de Desenvolvimento Científico e Tecnológico (CNPQ). VAMSAE received a master fellowship provided by Coordenação de aperfeiçoamento de Pessoal de Nıvel Superior (CAPES). LH received a PhD fellowship provided by Fundação de Amparo à Pesquisa do Estado do Rio de Janeiro (FAPERJ). JRC had no research funding upon the production of this manuscript. Coordenação de aperfeiçoamento de Pessoal de Nível Superior (CAPES) Finance Code 001.

ACKNOWLEDGMENTS

We thank the Centro Nacional de Biologia Estrutural e Bioimagem (CENABIO), in particular the Plataforma de High Content/throughput Analysis and Unidade de Microscopia Avançada (UMA), for providing an easily accessible infrastructure for research and for the detailed and insightful analysis of the data. To the Unidade de Microscopia Multiusuário (UNIMICRO) of the Instituto de Microbiologia Paulo de Góes (IMPG), in particular to technologist Jefferson Cypriano, for preparing the samples for SEM. And to the Plataforma de Equipamentos Multiusuários do Campus Duque de Caxias (PEM-CDC) for allowing the use of Scanning/Scanning-Transmission Electron Microscopy - Tescan VEGA 3 LMU free of charge. We would like to thank bioRxiv.org for allowing us to pre-publish this article (42).

SUPPLEMENTARY MATERIAL

The Supplementary Material for this article can be found online at: https://www.frontiersin.org/articles/10.3389/fviro.2022.908704/full#supplementary-material

REFERENCES

1. La Scola B, Audic S, Robert C, Jungang L, De Lamballerie X, Drancourt M, et al. A Giant Virus in Amoebae. *Science* (2003) 299:2033. doi: 10.1126/science.1081867
2. Schrad JR, Abrahão JS, Cortines JR, Parent KN. Structural and Proteomic Characterization of the Initiation of Giant Virus Infection. *Cell* (2020) 181:1046–61.e6. doi: 10.1016/j.cell.2020.04.032
3. dos Santos Oliveira J, Lavell AA, Essus VA, Souza G, Nunes GHP, Benício E, et al. Structure and Physiology of Giant DNA Viruses. *Curr Opin Virol* (2021) 49:58–67. doi: 10.1016/j.coviro.2021.04.012
4. Raoult D, Audic S, Robert C, Abergel C, Renesto P, Ogata H, et al. The 1.2-Megabase Genome Sequence of Mimivirus. *Science* (2004) 306:1344–50. doi: 10.1126/science.1101485
5. Legendre M, Santini S, Rico A, Abergel C, Claverie JM. Breaking the 1000-Gene Barrier for Mimivirus Using Ultra-Deep Genome and Transcriptome Sequencing. *Virol J* (2011) 8:99. doi: 10.1186/1743-422X-8-99
6. Aherfi S, Colson P, La Scola B, Raoult D. Giant Viruses of Amoebas: An Update. *Front Microbiol* (2016) 7:349. doi: 10.3389/fmicb.2016.00349
7. Colson P, La Scola B, Levasseur A, Caetano-Anollés G, Raoult D. Mimivirus: Leading the Way in the Discovery of Giant Viruses of Amoebae. *Nat Rev Microbiol* (2017) 15:243–54. doi: 10.1038/nrmicro.2016.197
8. Abrahão J, Silva L, Silva LS, Khalil JYB, Rodrigues R, Arantes T, et al. Tailed Giant Tupanvirus Possesses the Most Complete Translational Apparatus of the Known Virosphere. *Nat Commun* (2018) 9:1–12. doi: 10.1038/s41467-018-03168-1
9. Kuznetsov YG, Klose T, Rossmann M, McPherson A. Morphogenesis of Mimivirus and Its Viral Factories: An Atomic Force Microscopy Study of Infected Cells. *J Virol* (2013) 87:11200–13. doi: 10.1128/jvi.01372-13
10. Kuznetsov YG, Xiao C, Sun S, Raoult D, Rossmann M, McPherson A. Atomic Force Microscopy Investigation of the Giant Mimivirus. *Virology* (2010) 404:127–37. doi: 10.1016/j.virol.2010.05.007
11. Piacente F, Marin M, Molinaro A, De Castro C, Seltzer V, Salis A, et al. Giant DNA Virus Mimivirus Encodes Pathway for Biosynthesis of Unusual Sugar 4-Amino-4,6-Dideoxy-D-Glucose (Viosamine). *J Biol Chem* (2012) 287:3009–18. doi: 10.1074/jbc.M111.314559
12. Piacente F, De Castro C, Jeudy S, Gaglianone M, Laugieri ME, Notaro A, et al. The Rare Sugar N-Acetylated Viosamine is a Major Component of Mimivirus Fibers. *J Biol Chem* (2017) 292:7385–94. doi: 10.1074/jbc.M117.783217
13. Parakkottil Chothi M, Duncan GA, Armirotti A, Abergel C, Gurnon JR, Van Etten JL, et al. Identification of an L-Rhamnose Synthetic Pathway in Two Nucleocytoplasmic Large DNA Viruses. *J Virol* (2010) 84:8829–38. doi: 10.1128/jvi.00770-10
14. Boyer M, Azza S, Barrassi L, Klose T, Campocasso A, Pagnier I, et al. Mimivirus Shows Dramatic Genome Reduction After Intraamoebal Culture. *Proc Natl Acad Sci USA* (2011) 108:10296–301. doi: 10.1073/pnas.1101118108
15. Notaro A, Couté Y, Belmudes L, Laugeri ME, Salis A, Damonte G, et al. Expanding the Occurrence of Polysaccharides to the Viral World: The Case of Mimivirus. *Angew Chem* (2021) 133:20050–7. doi: 10.1002/ange.202106671
16. Rodrigues RAL, dos Santos Silva LK, Dornas FP, de Oliveira DB, Magalhães TFF, Santos DA, et al. Mimivirus Fibrils Are Important for Viral Attachment to the Microbial World by a Diverse Glycoside Interaction Repertoire. *J Virol* (2015) 89:11812–9. doi: 10.1128/jvi.01976-15
17. Ghigo E, Kartenbeck J, Lien P, Pelkmans L, Capo C, Mege JL, et al. Ameobal Pathogen Mimivirus Infects Macrophages Through Phagocytosis. *PLoS Pathog* (2008) 4. doi: 10.1371/journal.ppat.1000087
18. Oliveira G, La Scola B, Abrahão J. Giant Virus vs Amoeba: Fight for Supremacy. *Virol J* (2019) 16:1–12. doi: 10.1186/s12985-019-1244-3
19. Yaakov LB, Mutsafi Y, Porat Z, Dadosh T, Minsky A. Kinetics of Mimivirus Infection Stages Quantified Using Image Flow Cytometry. *Cytom Part A* (2019) 95:534–48. doi: 10.1002/cyto.a.23770
20. Ostrowski PP, Grinstein S, Freeman SA. Diffusion Barriers, Mechanical Forces, and the Biophysics of Phagocytosis. *Dev Cell* (2016) 38:135–46. doi: 10.1016/j.devcel.2016.06.023
21. Arandjelovic S, Ravichandran KS. Phagocytosis of Apoptotic Cells in Homeostasis. *Nat Immunol* (2015) 16:907–17. doi: 10.1038/ni.3253
22. Vaure C, Liu Y. A Comparative Review of Toll-Like Receptor 4 Expression and Functionality in Different Animal Species. *Front Immunol* (2014) 5:316. doi: 10.3389/fimmu.2014.00316
23. O'Neill LAJ, Golenbock D, Bowie AG. The History of Toll-Like Receptors-Redefining Innate Immunity. *Nat Rev Immunol* (2013) 13:453–60. doi: 10.1038/nri3446
24. Baizabal-Aguirre VM, Rosales C, López-Maciás C, Gómez MI. Control and Resolution Mechanisms of the Inflammatory Response 2016. *Mediators Inflamm* (2016) 2016:2–4. doi: 10.1155/2016/3591797
25. Khan M, La Scola B, Lepidi H, Raoult D. Pneumonia in Mice Inoculated Experimentally With Acanthamoeba Polyphaga Mimivirus. *Microb Pathog* (2007) 42:56–61. doi: 10.1016/j.micpath.2006.08.004
26. Saadi H, Pagnier I, Colson P, Cherif JK, Beji M, Boughalmi M, et al. First Isolation of Mimivirus in a Patient With Pneumonia. *Clin Infect Dis* (2013) 57:127–34. doi: 10.1093/cid/cit354
27. Zhang XA, Zhu T, Zhang PH, Li H, Li Y, Liu EM, et al. Lack of Mimivirus Detection in Patients With Respiratory Disease, China. *Emerg Infect Dis* (2016) 22:2011–2. doi: 10.3201/eid2211.160687
28. Reed LJ, Muench H. A SIMPLE METHOD OF ESTIMATING FIFTY PER CENT Endpoints12. *Am J Epidemiol* (1938) 27:493–7. doi: 10.1093/oxfordjournals.aje.a118408
29. Perkins ND. Integrating Cell-Signalling Pathways With NF-κb and IKK Function. *Nat Rev Mol Cell Biol* (2007) 8:49–62. doi: 10.1038/nrm2083
30. Günther J, Seyfert HM. The First Line of Defence: Insights Into Mechanisms and Relevance of Phagocytosis in Epithelial Cells. *Semin Immunopathol* (2018) 40:555–65. doi: 10.1007/s00281-018-0701-1
31. Chang D, Feng J, Liu H, Liu W, Sharma L, Dela Cruz CS. Differential Effects of the Akt Pathway on the Internalization of Klebsiella by Lung Epithelium and Macrophages. *Innate Immun* (2020) 26:618–26. doi: 10.1177/1753425920942582
32. García-Pérez BE, Mondragón-Flores R, Luna-Herrera J. Internalization of Mycobacterium Tuberculosis by Macropinocytosis in Non-Phagocytic Cells. *Microb Pathog* (2003) 35:49–55. doi: 10.1016/S0882-4010(03)00089-5
33. Olejnik J, Hume AJ, Mühlberger E. Toll-Like Receptor 4 in Acute Viral Infection: Too Much of a Good Thing. *PLoS Pathog* (2018) 14:1–7. doi: 10.1371/journal.ppat.1007390

34. Guillott L, Medjane S, Le-Barillec K, Balloy V, Danel C, Chignard M, et al. Response of Human Pulmonary Epithelial Cells to Lipopolysaccharide Involves Toll-Like Receptor 4 (TLR4)-Dependent Signaling Pathways: Evidence for an Intracellular Compartmentalization of TLR4. *J Biol Chem* (2004) 279:2712–8. doi: 10.1074/jbc.M305790200
35. Sender V, Stamme C. Lung Cell-Specific Modulation of LPS-Induced TLR4 Receptor and Adaptor Localization. *Commun Integr Biol* (2014) 7:1–9. doi: 10.4161/cib.29053
36. Lu YC, Yeh WC, Ohashi PS. LPS/TLR4 Signal Transduction Pathway. *Cytokine* (2008) 42:145–51. doi: 10.1016/j.cyto.2008.01.006
37. Thorley AJ, Grandolfo D, Lim E, Goldstraw P, Young A, Tetley TD. Innate Immune Responses to Bacterial Ligands in the Peripheral Human Lung - Role of Alveolar Epithelial TLR Expression and Signalling. *PLoS One* (2011) 6. doi: 10.1371/journal.pone.0021827
38. MacRedmond RE, Greene CM, Taggart CT, McElvaney NG, O'Neill S. Respiratory Epithelial Cells Require Toll-Like Receptor 4 for Induction of Human β-Defensin 2 by Lipopolysaccharide. *Respir Res* (2005) 6:1–11. doi: 10.1186/1465-9921-6-116
39. Silva LCF, Almeida GMF, Oliveira DB, Dornas FP, Campos RK, La Scola B, et al. A Resourceful Giant: APMV Is Able to Interfere With the Human Type I Interferon System. *Microbes Infect* (2014) 16:187–95. doi: 10.1016/j.micinf.2013.11.011
40. Almeida GMDF, Silva LCF, Colson P, Abrahao JS. Mimiviruses and the Human Interferon System: Viral Evasion of Classical Antiviral Activities, But Inhibition by a Novel Interferon-β Regulated Immunomodulatory Pathway. *J Interf Cytokine Res* (2017) 37:1–8. doi: 10.1089/jir.2016.0097
41. Miranda Boratto PVd, Pereira Andrade ACdS, Rodrigues RAL, La Scola B, Abrahão JS. The Multiple Origins of Proteins Present in Tupanvirus Particles. *Curr Opin Virol* (2019) 36:25–31. doi: 10.1016/j.coviro.2019.02.007
42. Oliveira J dos S, Oliveira DF, Essus VA, Nunes GHP, Honorato L, Oliveira L, et al. Paving the Way Towards Understanding the Inflammatory Pathways Triggered by Giant Viruses in Mammalian Cells: Effect of Mimivirus-Cell Interactions on Iκbα Degradation. *bioRxiv* (2021) 2021:1–21. doi: 10.1101/2021.09.16.460633

Conflict of Interest: The authors declare that the research was conducted in the absence of any commercial or financial relationships that could be construed as a potential conflict of interest.

Publisher's Note: All claims expressed in this article are solely those of the authors and do not necessarily represent those of their affiliated organizations, or those of the publisher, the editors and the reviewers. Any product that may be evaluated in this article, or claim that may be made by its manufacturer, is not guaranteed or endorsed by the publisher.